Λ-BARYON PRODUCTION IN $\pi^{\pm}$N INTERACTIONS

G. H. Arakelyan[1], C. Merino[2], and Yu. M. Shabelski[3]

Yerevan Physics Institute, Armenia

ABSTRACT

The process of Λ-baryon production in πp collisions is considered. The contribution of the string-junction mechanism to the strange baryon production in meson-baryon scattering is analysed. The results of numerical calculations in the framework of the Quark-Gluon String model are in reasonable agreement with the data.

[1]Permanent address: Yerevan Physics Institute, Armenia
E-mail: argev@mail.yerphi.am

[2]Permanent address: Departamento de Física de Partículas, Facultade de Física, and Instituto Galego de Altas Enerxías (IGAE), Universidade de Santiago de Compostela, Galicia, Spain
E-mail: merino@fpaxp1.usc.es

[3]Permanent address: Petersburg Nuclear Physics Institute, Gatchina, St.Petersburg, Russia
E-mail: shabelsk@thd.pnpi.spb.ru

1. INTRODUCTION

The Quark–Gluon String Model (QGSM) is based on the Dual Topological Unitarization (DTU) and it describes quite reasonably many features of high energy production processes, including the inclusive spectra of different secondary hadrons, their multiplicities, KNO–distributions, etc., both in hadron–nucleon and hadron–nucleus collisions [1, 2, 3, 4]. High energy interactions are considered as taking place via the exchange of one or several pomerons, and all elastic and inelastic processes result from cutting through or between those exchanged pomerons [5, 6]. The possibility of different numbers of pomerons to be exchanged introduces absorptive corrections to the cross-sections which are in agreement with the experimental data on production of hadrons consisting of light quarks. Inclusive spectra of hadrons are related to the corresponding fragmentation functions of quarks and diquarks, which are constructed using the reggeon counting rules [7].

In previous papers [8, 9] one has discussed the processes connected with the transfer of baryon charge over long rapidity distances. In the string models baryons are considered as configurations consisting of three strings attached to three valence quarks and connected in one point called "string junction" (SJ) [10, 11]. Thus the string-junction has a nonperturbative origin in QCD.

It is very important to understand the role of the SJ in the dynamics of high-energy hadronic interactions, in particular in processes implying baryon number transfer [12, 13, 14]. Significant results on this question were obtained in [8, 9]. The difference between [8] and [9] is only in the values of Regge intercept of SJ.

In the present paper we extend our study to the case of strange baryon production in πN interactions.

In references [8, 9] the SJ mechanism was mainly analyzed for proton production in πp and pp collisions, and strange baryon production in pp interaction. For the Λ production on pion beam were only considered the data on asymmetry.

Now we consider the data on spectra and new appeared data on asymmetry of Λ production on π-beam, not analysed in [8, 9]. For consideration we used both parametrisations of diquark fragmentation functions to strange baryons and Regge trajectory intercepts, as in [8, 9] (see sections 2 and 3 below).

In this paper we present a description of all available data and extract information on the properties of the SJ dynamics.

2. INCLUSIVE SPECTRA OF SECONDARY HADRONS IN QGSM

As it is thoroughly known, the exchange of one or several pomerons is one basic feature of high energy hadron–nucleon and hadron–nucleus interactions in the frame of QGSM and DPM. Each pomeron corresponds to a cylindrical diagram, and thus, when cutting a pomeron two showers of secondaries are produced . The inclusive spectrum of secondaries is determined by the convolution of diquark, valence, and sea quark distribution functions in the incident particle, $u(x, n)$, and the fragmentation functions of quarks and diquarks into secondary hadrons, $G(z)$.

The diquark and quark distribution functions depend on the number n of cut pomerons in a given diagram. In the following we will use the formalism of QGSM. In the case of a nucleon target the inclusive spectrum of a secondary hadron h has the form [1]:

$$\frac{x_E}{\sigma_{inel}} \frac{d\sigma}{dx} = \sum_{n=1}^{\infty} w_n \phi_n^h(x), \tag{1}$$

where x is the Feynman variable, and $x_E = 2E/\sqrt{s}$.

The probability for a process to have n cutted pomerons, w_n, has been extensively described using the quasieikonal approximation (see, for instance, [1, 6, 8]).

The function $\phi_n^h(x)$ represents the contribution of diagrams with n cut pomerons. In the case of a meson beam it has the form:

$$\phi_{\pi p}^h(x) = f_{\bar{q}}^h(x_+, n) \cdot f_q^h(x_-, n) + f_q^h(x_+, n) \cdot f_{qq}^h(x_-, n) + 2(n-1) f_s^h(x_+, n) \cdot f_s^h(x_-, n), \tag{2}$$

with

$$x_\pm = \frac{1}{2}\left[\sqrt{4m_T^2/s + x^2} \pm x\right], \tag{3}$$

where f_{qq}, f_q, and f_s correspond to the contributions of diquarks, valence quarks and sea quarks, respectively, and they are determined by the convolution of the diquark and quark distributions with the fragmentation functions, e.g.,

$$f_q^h(x_+, n) = \int_{x_+}^{1} u_q(x_1, n) \cdot G_q^h(x_+/x_1) dx_1. \tag{4}$$

The diquark and quark distributions, as well as the fragmentation functions, are determined from Regge intercepts [3, 4] (for the mathematical form of distribution functions see, for instance, [8]).

In the present paper we used the expression of the quark fragmentation functions into Λ given in [8, 9]:

$$G_u^\Lambda = G_d^\Lambda = a_{\bar{\Lambda}} (1-z)^{\lambda + \alpha_R - 2\alpha_B + \Delta\alpha} \cdot (1 + a_1 z^2)\ \ , G_u^{\bar{\Lambda}} = G_{\bar{d}}^\Lambda = (1-z) \cdot G_d^\Lambda, \tag{5}$$

with

$$\Delta\alpha = \alpha_\rho - \alpha_\phi = 1/2 \quad , \qquad \lambda = 2\alpha' < p_t^2 >= 0.5 \ . \tag{6}$$

Diquark fragmentation functions have more complicated forms. They contain two contributions. The first one corresponds to the central production of a $B\bar{B}$ pair, and has the form (see [8]):

$$G_{uu}^\Lambda = G_{ud}^\Lambda = G_{uu}^{\bar{\Lambda}} = G_{ud}^{\bar{\Lambda}} = a_{\bar{\Lambda}} (1-z)^{\lambda - \alpha_R + 4(1-\alpha_B) + \Delta\alpha}. \tag{7}$$

The second contribution is connected with the direct fragmentation of the initial baryon into the secondary one with conservation of the string junction. As discussed in [8, 9], three different types of such contributions exist, the secondary baryon consisting

of the SJ together with: a) two valence and one sea quarks, b) one valence and two sea quarks, or c) three sea quarks (see Fig. 2 in [8, 9]). The fraction of the incident baryon energy carried by the secondary baryon decreases from cases a) to c), whereas the mean rapidity gap between the incident and secondary baryon increases.

The probability to find a comparatively slow SJ in the case c) can be estimated from the data on $\bar{p}p$ annihilation into mesons (see [8]), where this probability, only experimentally known at low energies, turns out to be proportional to $s^{\alpha_{SJ}-1}$. However, it has been also argued [15] that the annihilation cross section contains a small component which is independent of s, making $\alpha_{SJ} \sim 1$.

The contribution of the term c) was analyzed in [8, 9], where its magnitude was taken proportional to a coefficient that we will denote by ϵ.

All the contributions are determined by equations similar to (2-4), with the corresponding fragmentation functions.

As it was noted above, we compare our calculations using the both parametrizations of fragmentation functions of diquarks into strange baryons and corresponding SJ trajectory intercepts α_{SJ}[8, 9].

In references [8, 9] were used the following expressions:

$$G^{\Lambda}_{ud} = a_N z^{\beta} \Big[v_0 \varepsilon (1-z)^2 + v_q z^{2-\beta}(1-z) + v_{qq} z^{2.5-\beta} \Big] (1-z)^{\Delta\alpha} \ , \ G^{\Lambda}_{uu} = (1-z) G^{\Lambda}_{ud}. \quad (8)$$

with $\beta = 1 - \alpha_{SJ}$.

The factor z^{β} is actually $z^{1-\alpha_{SJ}}$. As for the factor $z^{\beta} \cdot z^{2-\beta}$ in the second term, it is $2(\alpha_R - \alpha_B)$ [1]. For the third term one has just added an extra factor $z^{1/2}$.

In [8] the value $\alpha_{SJ} = 0.5$ was used, while in [9] $\alpha_{SJ} = 0.9$. The values of ϵ, v_0, v_q, and v_{qq} in (8) were taken from [8, 9]. All other model parameters were also taken from [1, 4, 8, 9].

The probabilities of transition into the secondary baryon of SJ without valence quarks, I_3, SJ plus one valence quark, I_2, and SJ plus a valence diquark, I_1, follow the simplest quark combinatorials [17]. Assuming the same strange quark suppression in all the cases, we obtain, for the relative yields of different baryons from SJ fragmentation without valence quarks:

$$I_3 = 4L^3 : 4L^3 : 12L^2S : 3LS^2 : 3LS^2 : S^3, \quad (9)$$

for secondary p, n, $\Lambda + \Sigma$, Ξ^0, Ξ^-, and Ω, respectively.

For I_2 we obtain

$$I_{2u} = 3L^2 : L^2 : 4LS : S^2 : 0, \quad (10)$$

and

$$I_{2d} = L^2 : 3L^2 : 4LS : 0 : S^2, \quad (11)$$

for secondary p, n, $\Lambda + \Sigma$, Ξ^0, and Ξ^-.

For I_1 we get

$$I_{1uu} = 2L : 0 : S, \tag{12}$$

and

$$I_{1ud} = L : L : S, \tag{13}$$

for secondary p, n, and $\Lambda + \Sigma$. The ratio S/L determines the strange suppression factor and $2L + S = 1$. In the numerical calculations we have used $S/L = 0.2$.

In agreement with empirical rules we assume that $\Sigma^+ + \Sigma^- = 0.6 \cdot \Lambda$ [18] in Eqs. (9)-(13). As customary Σ^0 are included into Λ. Note that the empirical rule used in many experimental papers is not consistent with the simplest quark statistics [19].

The values of v_0, v_q, and v_{qq} are directly determined by the corresponding coefficients of Eqs. (9)-(13), and by the probabilities to fragment a qqs system into $\Sigma^+ + \Sigma^-$ and Λ (see above).

For incident uu diquark and secondary Λ:

$$v_0 = \frac{12}{1.6} SL^2 \ \ , v_q = \frac{4}{1.6} SL \ \ , v_{qq} = \frac{1}{4} S \ ; \tag{14}$$

for incident ud diquark and secondary Λ:

$$v_0 = \frac{12}{1.6} SL^2 \ \ , v_q = \frac{4}{1.6} SL \ \ , v_{qq} = S \ . \tag{15}$$

As discussed above, although in the approach [10, 11] the baryon consists of three valence quarks together with SJ, which is conserved during the interaction, it has been argued [15] that the annihilation cross section contains a small component, which is independent of s and makes $\alpha_{SJ} \sim 1$. In any case, and with independence of the value of α_{SJ}, the graph corresponds to an annihilation contribution, and, therefore, it is weighted by a small coefficient which will be denoted by ε. In our calculation we will use both values of $\alpha_{SJ} = 0.5$ [8] and $\alpha_{SJ} = 0.9$ [9] and treat ε as a free parameter.

3. COMPARISON WITH THE DATA

The mechanism of the baryon charge transfer via SJ without valence quarks was not accounted for in papers [1, 2, 3, 4]. As it was shown in [8, 9] the data at comparatively low energies ($\sqrt{s} \sim 15 \div 40$ GeV) can be described with the values $\alpha_{SJ} = 0.5$ and $\varepsilon = 0.05$ (see [8]), or $\alpha_{SJ} = 0.9$ and $\varepsilon = 0.024$ [9].

The inclusive spectra of secondary Λ produced in πp collisions at energies 147 GeV/c [20] and 250 GeV/c [21, 22] are shown in Fig. 1 together with the curves calculated in the QGSM at 250 GeV for both values of α_{SJ}. The full line corresponds to $\alpha_{SJ} = 0.5$ [8], and the dashed line to $\alpha_{SJ} = 0.9$ [9]. The agreement of our results with the existing experimental data is quite reasonable, although one can see that at high values of $x_F > 0.6$, the theoretical curves have remarkable different behavior. Unfortunately, due to the absence of the experimental data one cannot distinguish between the two values of α_{SJ}.

The inclusive spectra of $\bar{\Lambda}$ produced in πp collisions at $E_{lab} = 250 GeV/c$ [21, 22] are shown in Fig. 2. The theoretical curves do not depend on the values of α_{SJ}.

The data on y-dependence of cross sections of Λ production at energies 100, 175, and 360 Gev/c [23], together with 250 GeV/c data [22] are compared with QGSM calculations in Fig. 3.

The model calculations were made for energies 100 and 360 GeV/c and both values of α_{SJ}: 1) dashed-dotted line corresponds to calculations for 360 Gev/c and $\alpha_{SJ} = 0.9$; 2) full line, for 360 Gev/c and $\alpha_{SJ} = 0.5$; 3) 100 Gev/c and $\alpha_{SJ} = 0.9$, and 4) 100 Gev/c and $\alpha_{SJ} = 0.5$. Some disagreements of the calculated curves with the data are of the same order as the disagreement among experimental data.

In the same way, the data on y-dependence of cross sections of $\bar{\Lambda}$ production at energies 100, 175, and 360 Gev/c from Ref. [23], together with 250 GeV/c data from Ref. [22] are shown in Fig. 4.

The spectra of antibaryons, produced in $\pi^- p$ collisions, Figs. 2 and 4, allow one to fix the fragmentation function of a quark into antibaryon. Since the fragmentation functions into $\bar{\Lambda}$ do not depend on the SJ contribution, the $\bar{\Lambda}$ spectra are the same when calculated with different values of α_{SJ}.

In Fig. 5 we show the data on the asymmetry of $\Lambda/\bar{\Lambda}$ produced in πp interactions at 250 GeV/c [24] and 500 GeV/c [25]. The asymmetry is defined as

$$A(B/\bar{B}) = \frac{N_B - N_{\bar{B}}}{N_B + N_{\bar{B}}}, \tag{16}$$

for each x_F bin.

The theoretical curves are calculated for 500 GeV/c with $\alpha_{SJ} = 0.5$ (full line) and $\alpha_{SJ} = 0.9$ (dashed line). Both calculations are in reasonable agreement with the existing data.

The data from reference [24], measured at rather large interval of x_F, were nott available during the preparation of this paper [8].

As we can see from the present calculations, the existing data on strange baryon production are reasonably compatible with both values of α_{SJ}. However, they show remarkably different behaviors for larger values of x_F in the forward hemisphere.

5. CONCLUSIONS

We have shown that experimental data on high-energy Λ production support the possibility of baryon charge transfer over large rapidity distances. The asymmetry is provided by string junction diffusion through baryon charge transfer.

The production of net baryons in πp interactions in the projectile hemisphere provides good evidence for such a mechanism.

As for the values of the parameters α_{SJ} and ε which govern the baryon charge transfer, we have seen that the data on strange baryon production at comparative low energies favor both the values $\alpha_{SJ} = 0.5$ and $\alpha_{SJ} = 0.9$.

The importance of understanding the dynamics of the transfer of baryon charge over large rapidity distances stresses the necesity of good experimental data in meson and baryon collisions with nucleons and nucleus, as well as in nucleus-nucleus interactions for different centralities.

For the Λ production on π beams the disagreement between the theoretical calculations for the two different values of $\alpha_{SJ} = 0.5, 0.9$, are within the experimental uncertainty.

Acknowledgments

The authors are thankful to A. Capella, C. Pajares, A. B. Kaidalov, and E. G. Ferreiro for useful discussions.

This work was partially financed by CICYT of Spain through contract FPA2002-01161, and by Xunta de Galicia through contract PGIDIT03PXIC20612PN.

G. H. Arakelyan and C.Merino were also supported by NATO grant CLG 980335 and Yu. M. Shabelski by grants NATO PDD (CP) PST.CLG 980287, RCGSS-1124.2003.2.

Figure Captions

Fig. 1. The experimental data on x_F spectra of secondary Λ in $\pi^{\pm}p$ collisions at 147 GeV/c [20] and 250 GeV/c [21, 22], together with QGMS description. The full line corresponds to calculations with $\alpha_{SJ} = 0.5$, while the dashed line corresponds to $\alpha_{SJ} = 0.9$.

Fig. 2. The x_F spectra of secondary $\bar{\Lambda}$ in πp collisions. Experimental data at 250 GeV/c [21, 22] and QGSM description.

Fig. 3. The y-dependence of spectra of secondary Λ in πp collisions. Experimental data at 100, 175, and 360 GeV/c [23], and 250 GeV/c[22]. The QGSM description at $E = 100$ and 360 Gev/c for both values of α_{SJ}.

Fig. 4. The y-dependence of spectra of secondary $\bar{\Lambda}$ in πp collisions. Experimental data at 100, 175, 360 GeV/c [23], and 250 GeV/c [22]. The QGSM description at $E = 100$ Gev/c (dashed line) and 360 Gev/c (full line).

Fig. 5. The QGSM description of the asymmetry $\Lambda/\bar{\Lambda}$ in $\pi^- p$ collisions at 500 GeV/c [25] and 250 GeV/c [24]. The curves were calculated for 500 GeV/c with $\alpha_{SJ} = 0.5$ (full line) and $\alpha_{SJ} = 0.9$ (dashed line).

References

[1] A. B. Kaidalov and K. A. Ter–Martirosyan, Yad. Fiz. **39**, 1545 (1984); **40**, 211 (1984);
A. B. Kaidalov and O. I. Piskunova, Yad. Fiz. **41**, 1278 (1985).

[2] A. Capella, U. Sukhatme, C. I. Tan, and J. Tran Thanh Van, Phys. Rep. **236**, 225 (1994);
A. Capella and J. Tran Thanh Van, Z. Phys. C**10**, 249 (1981).

[3] A. B. Kaidalov, K. A. Ter-Martirosyan and Yu. M. Shabelski, Yad. Fiz. **43**, 1282 (1986).

[4] Yu. M. Shabelski, Yad. Fiz. **44**, 186 (1986).

[5] V. A. Abramovski, V. N. Gribov, and O. V. Kancheli, Yad. Fiz.**18**, 595 (1973).

[6] K. A. Ter-Martirosyan, Phys. Lett. B**44**, 377(1973).

[7] A. B. Kaidalov, Sov. J. Nucl. Phys. **45**, 902 (1987); Yad. Fiz. **43**, 1282 (1986).

[8] G. H. Arakelyan, A. Capella, A. B. Kaidalov, and Yu. M. Shabelski, Eur. Phys. J. C**26**, 81 (2002).

[9] F. Bopp and Yu. M. Shabelski, hep-ph/0406158 (2004).

[10] M. Imachi, S. Otsuki, and F. Toyoda, Prog. Theor. Phys. **54**, 280 (1976); **55**, 551 (1976).

[11] G. C. Rossi and G. Veneziano, Nucl. Phys. B**123**, 507 (1977).
L. Montanet, G. C. Rossi, and G. Veneziano, Phys. Rep. **63**, 149 (1980).

[12] B. Z. Kopeliovich and B. G. Zakharov, Z. Phys. C**43**, 241 (1989).

[13] B. Z. Kopeliovich and B. G. Zakharov, Fiz. Elem. Chast. Atom. Nucl. **22**, 140 (1991).

[14] D. Kharzeev, Phys. Lett. B**378**, 238 (1996).

[15] B. Z. Kopeliovich and B. G. Zakharov, Phys. Lett. B**211**, 211 (1998);
E. Gotsman and S. Nusinov, Phys. Rev. D**22**, 624 (1980).

[16] B. Z. Kopeliovich and B. Povh, Z. Phys. C**75**, 693, (1997).

[17] A. Capella and C. A. Salgado, Phys. Rev. C**60**, 054906 (1999).

[18] H. Appelshauser et al. (NA49 Collaboration), Nucl. Phys. A**638**, 91c (1998).

[19] V. V. Anisovich, M. N. Kobrinsky, J. Nyiri, and Yu. M. Shabelski, Usp. Fiz. Nauk **144**, 553 (1984); *Quark Model and High Energy Collisions*, World Scientific, Singapore (1985).

[20] D. Brick et al., Nucl. Phys. B**164**, 1 (1980).

[21] I. V. Ajinenko et al., Z. Phys. J. C**44**, 573 (1989).

[22] D. Bogert et al., Phys. Rev. D**16**, 2098 (1977).

[23] N. N. Biswas et al., Nucl. Phys. B**167**, 41 (1980).

[24] G. A. Alves et al. (E769 Collaboration), hep-ex/0303027; Phys. Lett. B**559**, 179 (2003).

[25] E. M. Aitala et al. (E791 Collaboration), hep-ex/0009016, Phys. Lett. B**496**, 9 (2000).

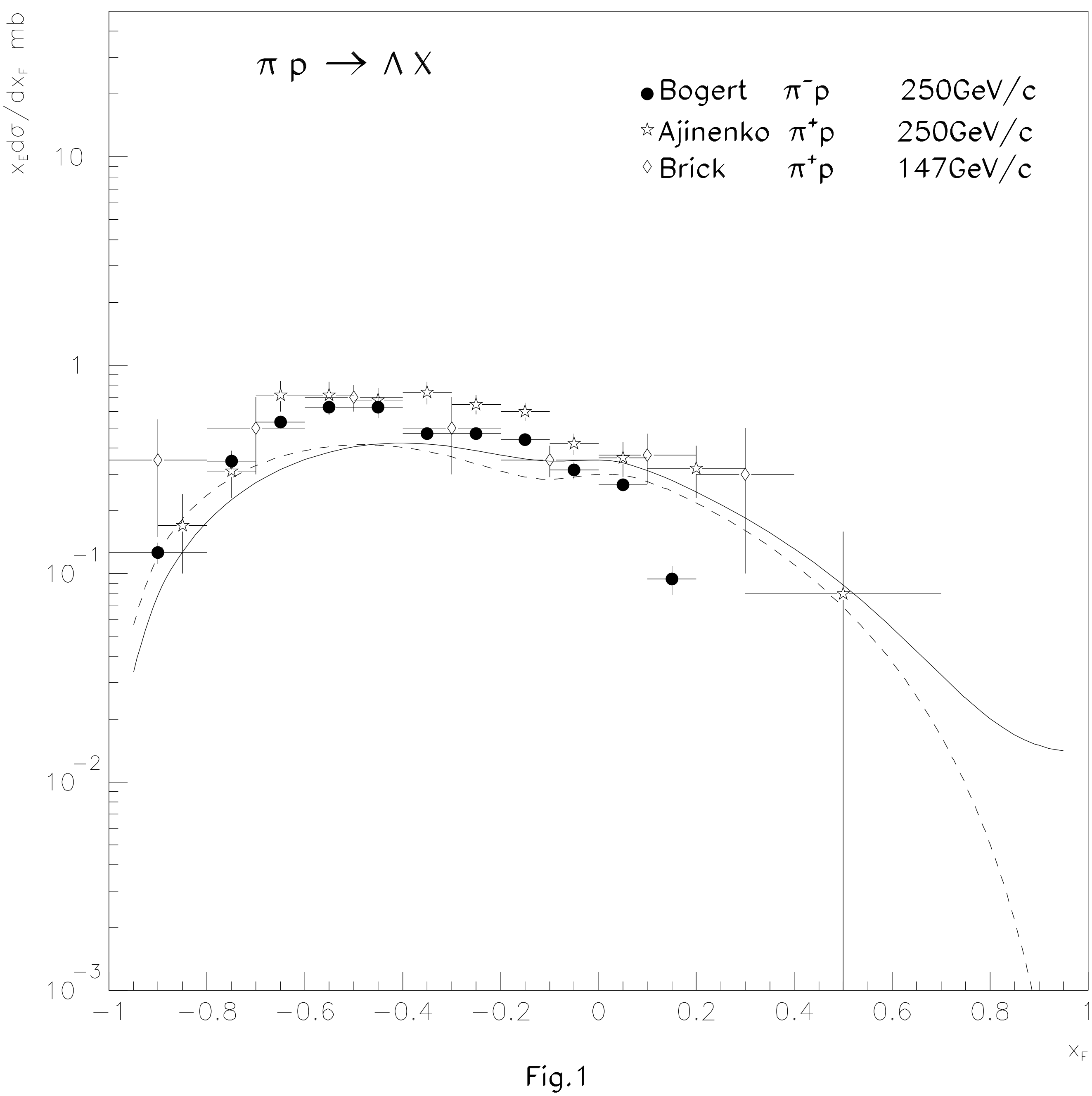

$x_E d\sigma/dx_F$ mb
$\pi\, p \rightarrow \Lambda\, X$
Bogert $\pi^- p$ 250GeV/c
Ajinenko $\pi^+ p$ 250GeV/c
Brick $\pi^+ p$ 147GeV/c
10
1
10^{-1}
10^{-2}
10^{-3}
−1
−0.8
−0.6
−0.4
−0.2
0
0.2
0.4
0.6
0.8
1
x_F

Fig.1

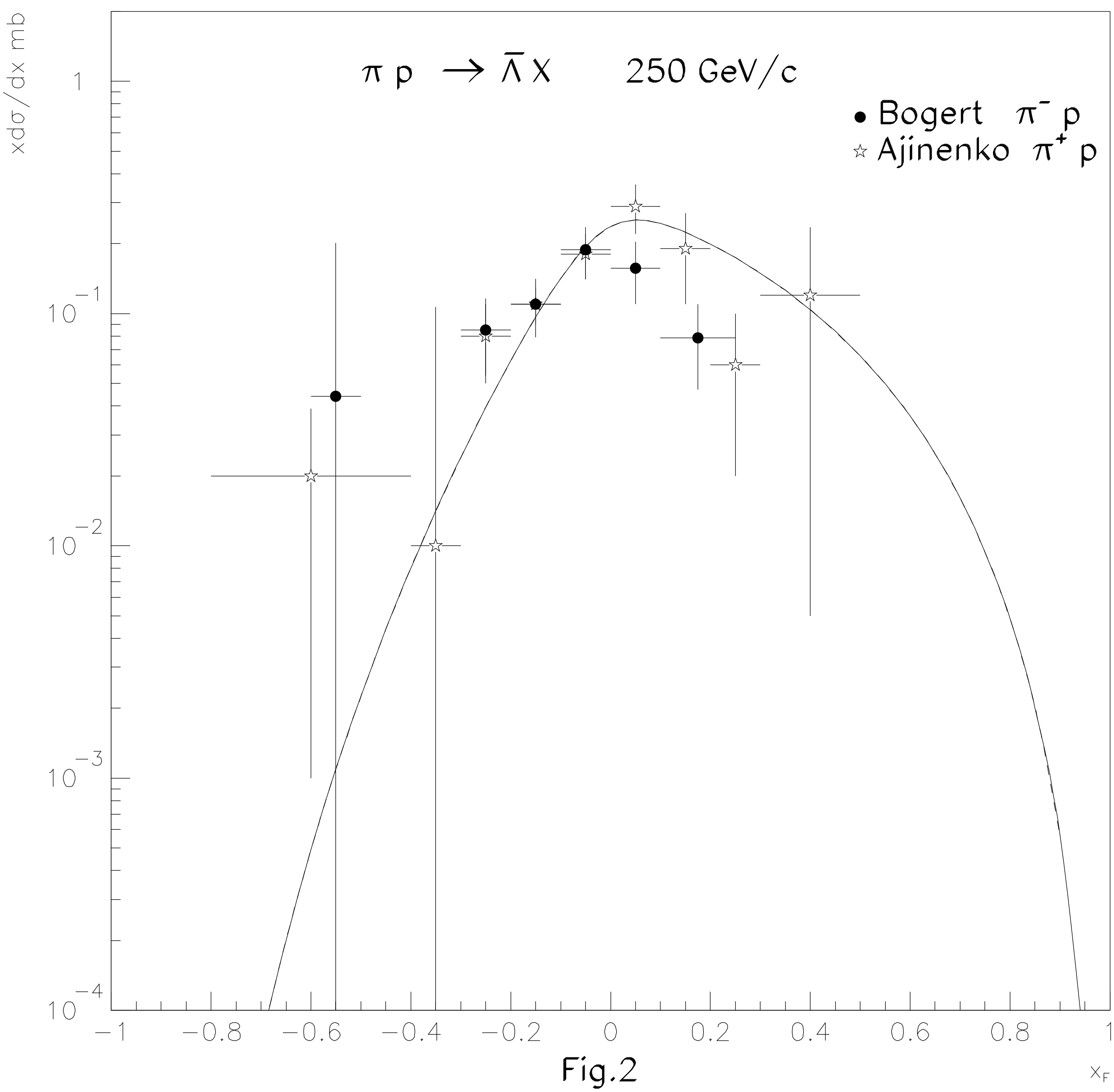

$\pi\, p \rightarrow \bar{\Lambda} X$ 250 GeV/c
Bogert $\pi^- p$
Ajinenko $\pi^+ p$
xdσ/dx mb
1
10^{-1}
10^{-2}
10^{-3}
10^{-4}
−1
−0.8
−0.6
−0.4
−0.2
0
0.2
0.4
0.6
0.8
1
x_F

Fig.2

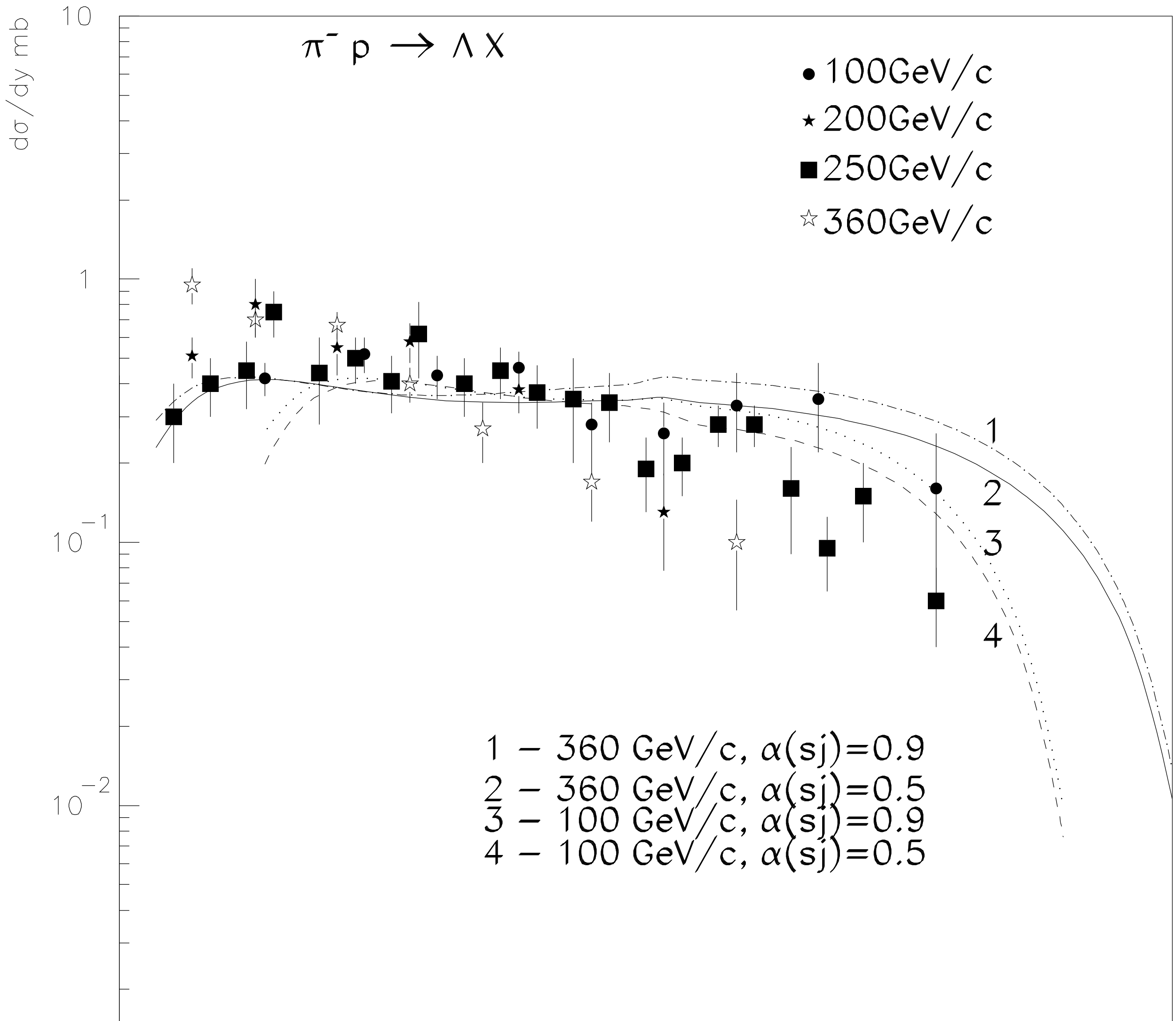

dσ/dy mb
π⁻ p → Λ X
100GeV/c
200GeV/c
250GeV/c
360GeV/c
1
2
3
4
1 – 360 GeV/c, α(sj)=0.9
2 – 360 GeV/c, α(sj)=0.5
3 – 100 GeV/c, α(sj)=0.9
4 – 100 GeV/c, α(sj)=0.5
y

Fig.3

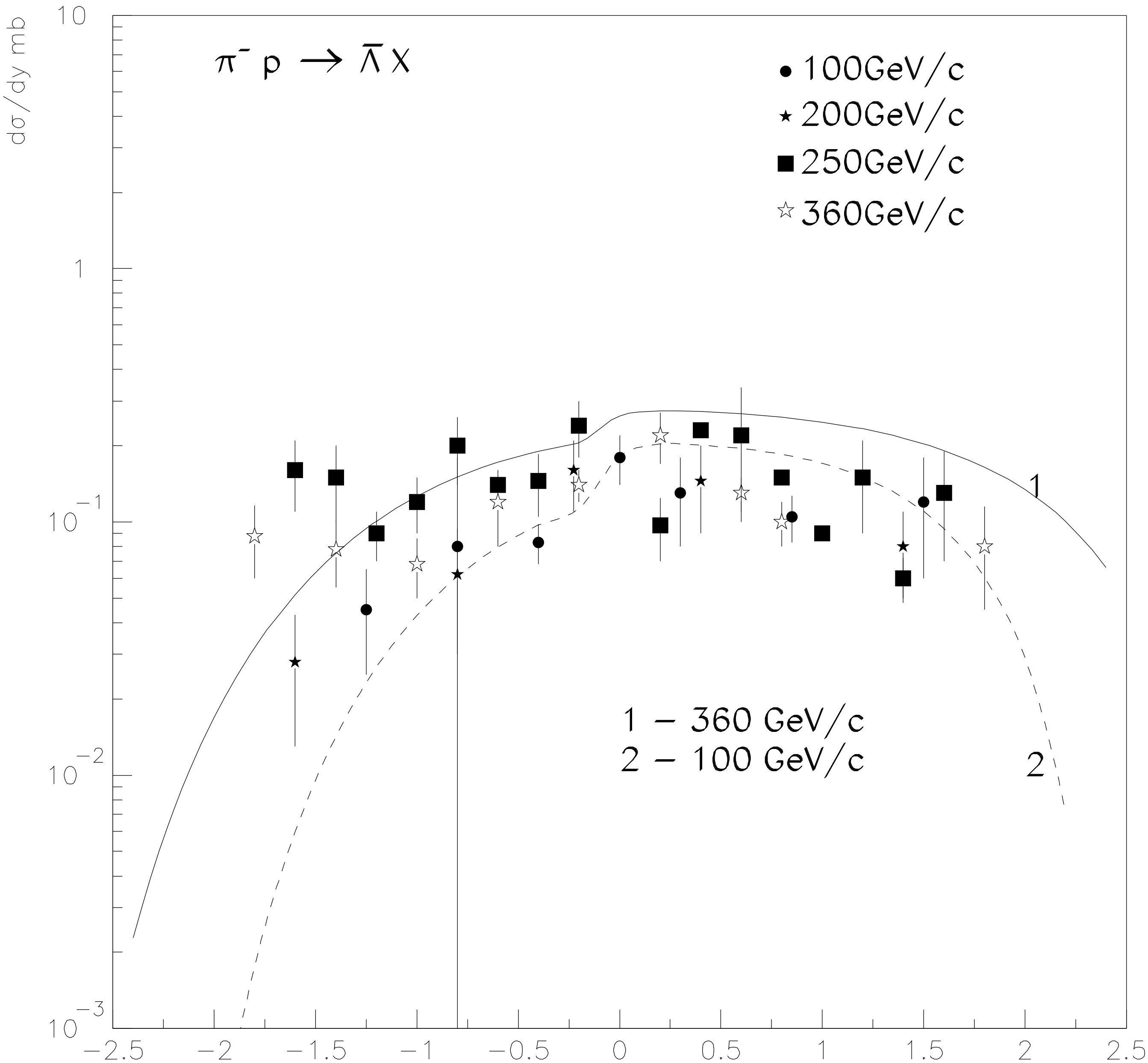

10
1
10^{-1}
10^{-2}
10^{-3}
dσ/dy mb
$\pi^- p \rightarrow \bar{\Lambda} X$
100GeV/c
200GeV/c
250GeV/c
360GeV/c
1 – 360 GeV/c
2 – 100 GeV/c
1
2
−2.5 −2 −1.5 −1 −0.5 0 0.5 1 1.5 2 2.5
y

Fig.4

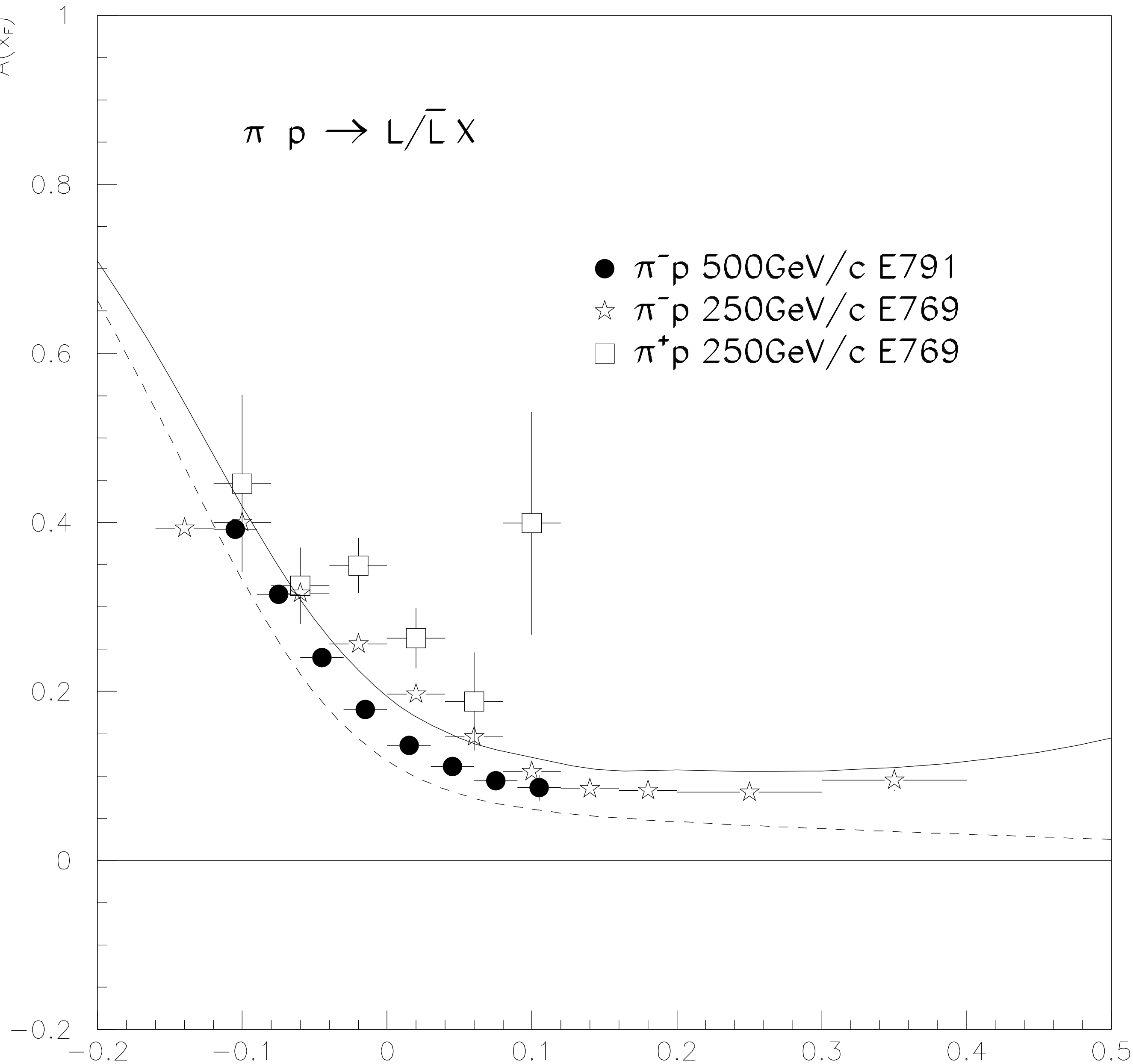

A(x_F)
π p → L/L̄ X
π⁻p 500GeV/c E791
π⁻p 250GeV/c E769
π⁺p 250GeV/c E769
1
0.8
0.6
0.4
0.2
0
−0.2
−0.2
−0.1
0
0.1
0.2
0.3
0.4
0.5
x_F

Fig.5